 

*LASER SPECTROSCOPY*

PACS numbers: 42.55.Px; 42.62.Fi; 33.20.–t
DOI: 10.1070/QE2014v044n10ABEH015319

# Investigation of broadening and shift of vapour absorption lines of $H_2{}^{16}O$ in the frequency range 7184–7186 $cm^{-1}$

A.I. Nadezhdinskii, A.A. Pereslavtseva, Ya.Ya. Ponurovskii

***Abstract.*** **We present the results of investigation of water vapour absorption spectra in the 7184–7186 $cm^{-1}$ range that is of particular interest from the viewpoint of possible application of the data obtained for monitoring water vapour in the Earth's stratosphere. The doublet of $H_2{}^{16}O$ near $\nu$ = 7185.596 $cm^{-1}$ is analysed. The coefficients of broadening and shift of water vapour lines are found in the selected range in mixtures with buffer gases and compared to those obtained by other authors.**

***Keywords:*** *diode laser, water molecule, parameters of line broadening and shift.*

## 1. Introduction

Precise measurement of absorption spectra of water vapour in the near-IR range is an important problem especially under the conditions of the increasing greenhouse effect. Water vapour is one of the main gases involved in this effect which is responsible for the transfer of solar radiation in the Earth's atmosphere. Unfortunately, present information about absorption of radiation by water molecules in the near-IR range is not complete and precise. First of all, this is explained by a sufficiently complicated structure of absorption spectra in this range due to overlapping of composite and Raman bands.

Many works are devoted to studying a fine rotational structure of absorption spectra of water vapour in the near-IR wavelength range. Here we may mention most remarkable and complete works [1–8]. Thus, Lepère et al. [4] used a three mirror cell in a stabilised diode laser spectrometer for investigating the profiles of water vapour lines near the frequency of 7185.59 $cm^{-1}$. They employed model Voigt, Galatry and Rautian–Sobelman profiles for analysing the lines. A Fourier spectrometer was employed in [5–8] for obtaining high-resolution (0.01–0.02 $cm^{-1}$) spectra of the gas mixture comprising HDO, $D_2O$, $H_2O$. In the 6000–7700 $cm^{-1}$ range, 2445 lines of HDO were detected which belong to the bands (101)–(000), (021)–(000), (210)–(000) and (002)–(000) [7]. The fine rotational structure of vapour spectra of water with natural isotopic contents in the near-IR range was most completely identified in [9–11] by means of Fourier spectroscopy and the cw-cavity ring down spectroscopy (CW-CRDS). The spectral range of 6885–7408 $cm^{-1}$, which corresponds to a first hexad of interacting vibrational–rotational bands of $H_2O$, was investigated and the frequencies and intensities of more than 12 700 lines were determined. This made it possible to substantially correct spectral databases (HITRAN, GEISHA, etc).

In this paper we present the results of investigation of water vapour absorption spectra in the frequency range of 7184–7186 $cm^{-1}$. This range is of particular interest because the data obtained may help monitoring water vapour in the Earth's stratosphere. The $H_2{}^{16}O$ doublet which comprises the vibrational–rotational lines $6_{61} \leftarrow 6_{60}$ of the band $\nu_1 + \nu_3$ and $5_{23} \leftarrow 6_{16}$ of the band $2\nu_1$ is analysed. The coefficients of broadening and shift for these lines in collisions with buffer gas molecules are found and compared with the results obtained by other authors [4, 7].

## 2. Experimental setup

The absorption lines of water vapour in the spectral range of diode laser (DL) tuning were investigated on an experimental setup shown schematically in Fig. 1.

The experimental setup is a two-channel diode laser spectrometer with the reference and analytical channels and a pre-evacuation system for filling, evacuating and preparing gas

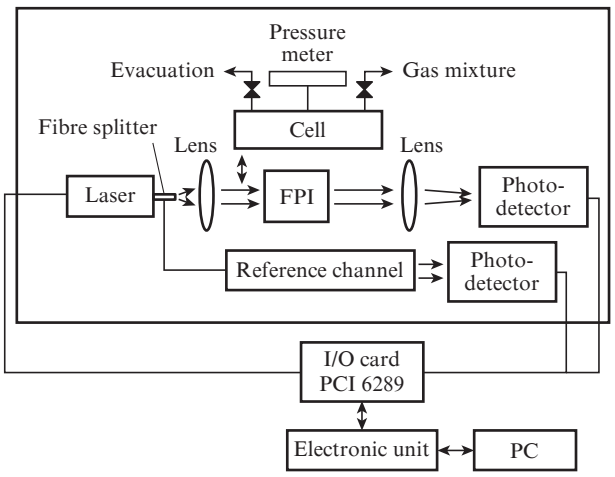


**Figure 1.** Schematic diagram of the experimental setup.

**A.I. Nadezhdinskii, Ya.Ya. Ponurovskii** A.M. Prokhorov General Physics Institute, Russian Academy of Sciences, ul. Vavilova 38, 119991 Moscow, Russia;
**A.A. Pereslavtseva** A.M. Prokhorov General Physics Institute, Russian Academy of Sciences, ul. Vavilova 38, 119991 Moscow, Russia; Moscow Institute of Physics and Technology, Institutskii per. 9, 141700 Dolgoprudnyi, Moscow region, Russia; e-mail: nastyushk@inbox.ru

Received 24 September 2013, revision received 14 January 2014
Kvantovaya Elektronika **44** (10) 950–956 (2014)
Translated by N.A. Raspopov

mixtures for the analytical cell. The reference channel is used for stabilising the temperature during the DL pumping current scanning cycles by the absorption line of the investigated gas and for absolute frequency calibration of absorption spectra. The channel comprises the cell with a length of 20 cm and volume of 25 mL filled with the (reference) gas in question. The cell windows are made of S-52 glass (molybdenum glass) and have a wedge with the angle of 1.5° for preventing the interference effects of laser radiation. The pressure of the water vapour inside the cell at a temperature of 25 °C was 13 mbar. The cell was hermetically sealed.

In the analytical channel, a vacuum optical cell of length $199.8 \pm 0.2$ cm was placed with a gas mixture under study. Stainless steel with the polished internal surface was used to fabricate the cell and its windows of 30 mm in diameter were made of high-temperature $CaF_2$ glass in the form of wedges with an angle of 7′. A temperature sensor for instantaneous measurement of the temperature of external surface of the cell was mounted on the cell housing. There were also two pressure sensors: Elemer [12] (with the measurement range of 0–1000 mbar and measurement error of 0.2%) and Sensor [13] (with the measurement range of 0–100 mbar and measurement error of 0.1%). A Fabry–Perot interferometer (FPI) was used for alignment of the frequency scale of absorption spectra. It was a quartz resonator with partially deposited faces for producing a high-quality interference pattern (with the free spectral range $\Delta\lambda/\lambda^2 = 1/(2L_{FPI}n_{FPI}) = 0.04922(2)$ cm$^{-1}$, where $L_{FPI} = 69.39(4)$ mm, and $n_{FPI}$ is the refractive index of the FPI material). The output radiation beam from the laser was made parallel and focused to a photodetector by lenses. As photodetectors, pin-diodes (Hamamatsu) [14] were used with the diameter of active area 2.0 mm and detection ability of $5\times10^{12}$ cm Hz$^{1/2}$ W$^{-1}$. A maximal spectral response at the wavelength of 1.7 μm was 1.1 A W$^{-1}$.

The preamplifiers of the reference and analytical channels had the following parameters: the conversion coefficient and bandwidth were 10 V mA$^{-1}$ and 120 kHz, respectively.

Absorption spectra of water vapour were investigated by using a diode laser (NTT Electronics) [15] with a central radiation frequency of 1.39253 μm and a single-mode fibre output. The output optical power was 30 mW, the threshold pumping current was 10 mA, the maximal current was 120 mA and the tuning range was 10 nm. The temperature stabilisation system of the DL based on a thermistor and a Peltier thermoelectric heatsink provided the temperature variation of the active element from 2 to 55 °C with temperature instability of $2\times10^{-4}$ °C. The temperature stabilisation system realised the proportional-plus-integral operation and the additional regime of temperature stabilisation by the absorption line of the reference gas.

The control and data acquisition system of the diode-laser spectrometer (DLS) comprised a 16-bit input/output card 6289 (National Instruments) with the sampling rate of 333 kHz, two ADC channels and eight-channel differential ADC. The card was a multiplexed one and therefore the resulting sampling rate in our experiments was 111 kHz.

The optical cell was connected through vacuum valves to the forevacuum system which is schematically shown in Fig. 2. The forevacuum unit was employed to evacuate optical cells and to prepare mixtures of various compositions. This unit comprised a DP-5 differential pressure sensor (measurement range 0–133.3 mbar, error 0.5%), standard pressure gauge and VT-2A-P thermocouple vacuum gauge (measurement range 0.0013–0.267 mbar). The total internal volume of the system was 150 mL.

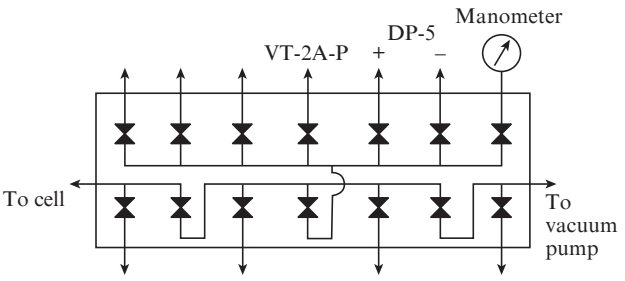


**Figure 2.** Schematic diagram of the forevacuum system.

## 3. DLS characteristics

Typical signals from DLS photodetectors are presented in Fig. 3. In accumulating and averaging the sample comprising 20 absorption spectra of gases under investigation, the signal-to-noise ratio was above $10^4$ at the characteristic time of sample averaging of 2 s. The spectral resolution of the DLS equal to $2\times10^{-4}$ cm$^{-1}$ was determined by the width of the instrumental function of the spectrometer, which was directly connected with the width of the DL generation line. The error of finding the centre of the Doppler-broadened absorption line was no greater than $2\times10^{-5}$ cm$^{-1}$ and was determined by the accuracy of fitting the line profile to model spectra.

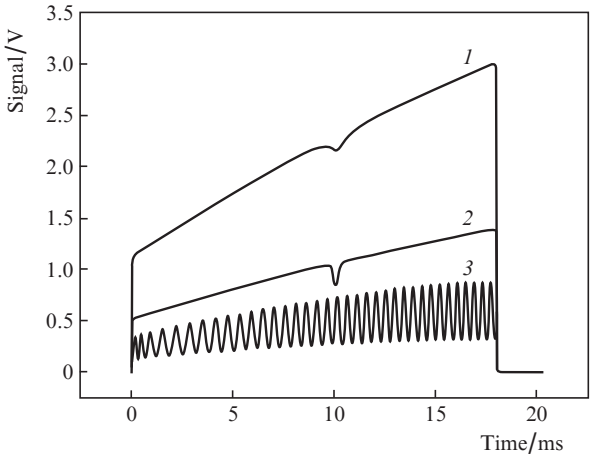


**Figure 3.** Typical signals from photodetectors of a two-channel DLS recording radiation: (*1*) passed through the cell, (*2*) passed through the analytical cell and (*3*) FPI.

Noise of the DLS optoelectronic section was investigated by using the Allan variance technique [16], which determines the square root from the dispersion of the measured parameter as a function of the averaging time. The Allan variances for the optical density $D$ and temperature of the DL active element, measured in the cell of length 2 m with no absorbing gas inside, are shown in Fig. 4. One can see that at the accumulation time of 4 s the minimal detectable value of the optical density reaches $8\times10^{-6}$ and the temperature instability in this case is $4\times10^{-5}$ °C. At a longer accumulation time the drift of the measured value of $D$ is observed. It is caused by fluctuations of the detected signal in the absence of the absorption gas in the cell (the base line of the DL) and by other factors which affect the accuracy of the experiment (tempera-

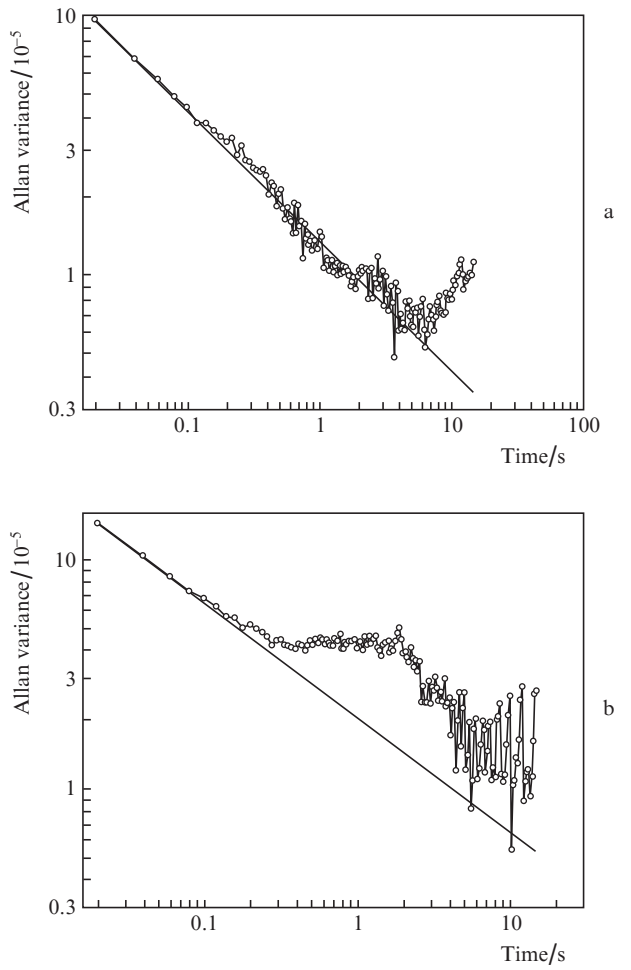


**Figure 4.** Allan variances for (a) the optical density inside cell and (b) for temperature of the DL active element.

ture, gas pressure, etc.). Allan variances for the optical density and temperature should be taken into account in long-term measurements of absorption line profiles.

For the noise characteristics of the spectrometer to be investigated, we also analysed the sources of noise related to the interference of laser radiation on the surfaces of mirrors and cell windows (secondary sources of interference). Specific features of image formation on the mirrors and cell windows, as well as imperfect mirrors, used in the installation result in a parasitic interference, which affects the noise level of the spectrometer [17]. For investigating the role of secondary sources of interference we used the dependence of the fast Fourier transform of the output signal on a distance between the DL and source of the secondary radiation, which interferes with the basic DL radiation in the evacuated cell of length 2 m. This dependence is presented in Fig. 5. The peaks corresponding to distances 30 (reflection from the input windows of the cell), 114 (reflection inside the cell) and 200 cm (reflection

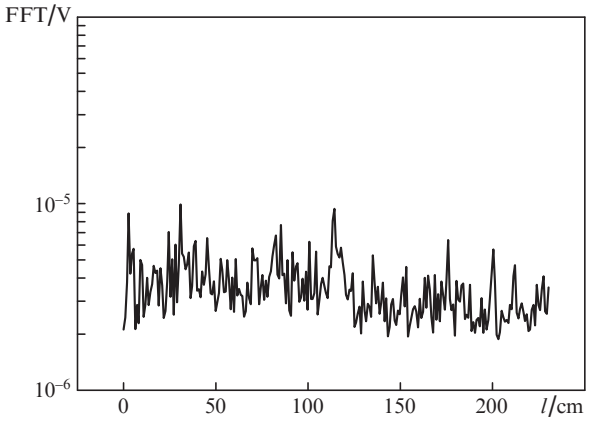


**Figure 5.** Fast-Fourier transform (FFT) of the output signal vs. the distance $l$ between the DL and source of secondary radiation interfering with the primary radiation of the DL in the evacuated cell of length 2 m.

from the output window of the cell) are clearly seen. Influence of these sources on the spectrometer sensitivity results in that the noise level reaches $1\times10^{-5}$. Such a noise level yields the error comparable with existing systematic errors of the experiment (temperature and pressure inaccuracy), and hence no special suppression of interference noise was performed.

## 4. Measurements of intensity of absorption lines of $H_2{}^{16}O$ vapour near $\lambda$ = 1.392 μm

The tuning range of the DL includes lines with the central frequencies 7185.597 cm$^{-1}$ (Q-branch, band $\nu_1+\nu_3$, transition $6_{61}\leftarrow6_{60}$) and 7185.394 cm$^{-1}$ (P-branch, band $2\nu_1$, transition $5_{23}\leftarrow6_{16}$). The parameters of the investigated lines taken from the spectral database HITRAN-2008 [18] are presented in Table 1.

The error of determining line intensities is no greater than 10% and uncertainty of finding line centres varies from 0.01 to 0.001 cm$^{-1}$. Figure 6 presents a model spectrum of water vapour near $\lambda$ = 1.39 μm, which was obtained by using data from HITRAN-2008.

The installation described above (Fig. 1) was used for obtaining the absorption spectra of water vapour in the range 7184–7186 cm$^{-1}$. The cell of length 2 m was filled with water vapour at a temperature of 23 °C. The pressure of water vapour varied from 0.15 to 11 mbar. Prior to recording a spectrum, the cell was cleaned by dry nitrogen and evacuated; then, the base line (line of zero absorption) was recorded. The experiments were controlled by a specially written programme. Figure 7 shows the experimental spectra of water vapour without a buffer gas.

The intensities of absorption water vapour lines under the conditions of broadening by a native gas were found by using the 'hard-collision' model (Rautian–Sobelman profile [19]), because the Voigt model, which neglects the effects of line narrowing in collisions of molecules, is not correct in this

**Table 1.** Parameters of investigated lines taken from HITRAN-2008 spectral database [18].

| $\nu_0$/cm$^{-1}$ | Transition | $S_0$/cm$^{-2}$ atm$^{-1}$ | $\gamma^0_{air}$/cm$^{-1}$ atm$^{-1}$ | $\gamma^0_{H_2O}$/cm$^{-1}$ atm$^{-1}$ | $E$/cm$^{-1}$ | $n$ | $\delta$/cm$^{-1}$ atm$^{-1}$ |
|---|---|---|---|---|---|---|---|
| 7185.394 | $2\nu_1$, $6_{16}\rightarrow5_{23}$ | 0.001279 | 0.0924 | 0.435 | 447.25 | 0.72 | –0.00892 |
| 7185.597 | $\nu_1+\nu_3$, $6_{60}\rightarrow6_{61}$ | 0.019701 | 0.0413 | 0.195 | 1045.1 | 0.19 | –0.01346 |

Note: $\nu_0$ is the frequency of the line centre; $S_0$ is the line intensity; $\gamma^0_{air}$, $\gamma^0_{H_2O}$ are the coefficients of broadening in air and in native vapours of $H_2O$; $E$ is the lower level energy; $n$ is the coefficient of a temperature dependence (exponent); $\delta$ is the shift coefficient.

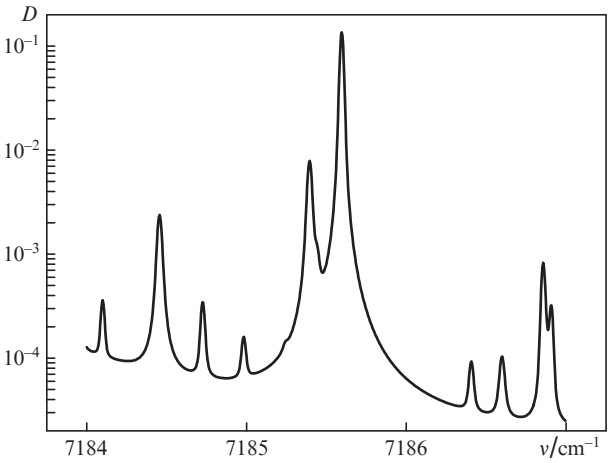


**Figure 6.** Model spectrum of the absorption lines of water vapour near 1.39 μm in the cell of length 2 m at the pressure of 101.3 mbar; the concentration of water vapour is 10%, the temperature is 23 °C.

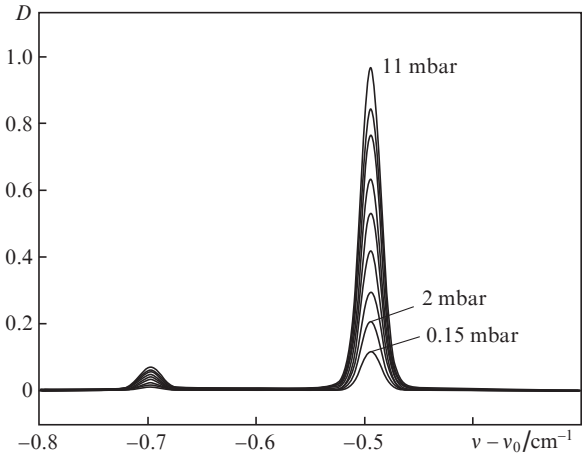


**Figure 7.** Experimental spectra of water vapour at various pressures without a buffer gas. The pressure varies from 0.15 to 11 mbar; the cell length is 2 m.

case. The profile of the absorption line in the model chosen has the form

$$k(\nu - \nu_0) = A\,\mathrm{Re}\left[\frac{W(x,y+z)}{1-\sqrt{\pi}z\,W(x,y+z)}\right], \tag{1}$$

where $\nu_0$ is the line centre frequency;

$$W(x,y) = \frac{\mathrm{i}}{\pi}\int_{-\infty}^{+\infty}\frac{\exp(-t^2)}{x-t+\mathrm{i}y}\,\mathrm{d}t \tag{2}$$

is the complex probability function;

$$x = \sqrt{\ln 2}\,\frac{\nu-\nu_0}{\gamma_\mathrm{D}};\quad y = \sqrt{\ln 2}\,\frac{\gamma_\mathrm{L}}{\gamma_\mathrm{D}};$$
$$z = \sqrt{\ln 2}\,\frac{\zeta}{\gamma_\mathrm{D}}; \tag{3}$$

$\gamma_\mathrm{L}$ is the half width at half maximum of the Lorentzian profile;

$$\gamma_\mathrm{D} = 3.5812\times10^{-7}\sqrt{\frac{T}{M}}\,\nu_0 \tag{4}$$

is the half width at half maximum of the Doppler profile; $\zeta = \zeta^0 P$ is the Dicke narrowing parameter, which characterises the efficient frequency of collisions; $P$ is the buffer gas pressure; $\zeta^0$ is the coefficient of narrowing (in $\mathrm{cm^{-1}\,atm^{-1}}$); $T$ is the temperature; and $M$ is the molecular mass.

The parameter $z$ describes the change of the particle velocity in a collision, which should reduce the contribution of Doppler broadening.

For approximating line profiles by the Rautian–Sobelman model, the software was used which was capable of operating with line multiplets [20]. The fitting procedure was performed in the 'line-by-line' regime where each experimental point of the absorption coefficient was a sum of additive contributions from absorption coefficients of each line residing in the fitting spectral range. Four parameters were varied for each line: intensity, frequency shift, collisional half-width and Dicke narrowing parameter. The Doppler contribution to the line width was fixed and calculated by formula (4).

Processing of line profiles of water vapour yields the line intensities (see Table 2). The intensity of the stronger line at $\nu = 7185.597\ \mathrm{cm^{-1}}$ coincides with results of other authors within the measurement accuracy. For the line at $\nu = 7185.394\ \mathrm{cm^{-1}}$ the measured intensity is above the results of the cited works. It may be explained by the fact that in those works an additional line at $\nu = 7185.400\ \mathrm{cm^{-1}}$ was analysed and its intensity was $2.7\times10^{-3}\ \mathrm{cm^{-1}\,atm^{-1}}$, that is, the intensities also differ by $\sim10^{-3}$.

**Table 2.** Intensities of $H_2O$ doublet lines obtained in the present and other works.

| Transition | $S_0/10^{-3}\ \mathrm{cm^{-2}\,atm^{-1}}$ | | | |
|---|---|---|---|---|
| | Present work | [4] | [18] | [7] |
| $6_{60}\leftarrow6_{61}$ *,** 7185.597 $\mathrm{cm^{-1}}$ | 19.2(6) | 19.5(3) | 20(1) | 18.8(4) |
| $5_{23}\leftarrow6_{16}$ *** 7185.394 $\mathrm{cm^{-1}}$ | $15.1(2)\times10^{-1}$ | $13.1(6)\times10^{-1}$ | $13(1)\times10^{-1}$ | $11(1)\times10^{-1}$ |

* Actually, this line is the unresolved $K_a$-doublet of the two lines $6_{60}\leftarrow6_{61}$ (strong) and $6_{61}\leftarrow6_{60}$ (weak) with the splitting of less than 0.001 $\mathrm{cm^{-1}}$. The intensity from [4] given in the table is the net intensity of these two lines. ** One more line at $\nu = 7185.575\ \mathrm{cm^{-1}}$ corresponding to the transition $6_{16}\leftarrow5_{23}$ of the vibration branch (200)←(000) is found in [4] with the intensity of $0.3\times10^{-3}\ \mathrm{cm^{-2}\,atm^{-1}}$. *** This transition belongs to the vibration branch (200)←(000) and the rest transitions belong to the branch (101)←(000).

From the absorption spectra of water vapour experimentally recorded in the range mentioned above, we estimated the width of the DL generation line ($\gamma_\mathrm{gen}$) related with fluctuations of the emission frequency. The procedure of determining the width of the generation line comprised the fitting of the narrow Doppler-broadened absorption line of $H_2O$ to the profile $\mathrm{Re}(W(x,y))$ (2) and determination of the Lorentz component $\gamma_\mathrm{L}$. The Doppler part of the line width $\gamma_\mathrm{D}$ ($\mathrm{cm^{-1}}$) in this case should coincide with its theoretical value for a given gas temperature. The fitting procedure yields $\gamma_\mathrm{gen} = 0.00016(1)\ \mathrm{cm^{-1}}$ (5.3 MHz), which well agrees with data on the width of the generation line for a distributed feedback DL.

## 5. Broadening and shift of water double line $H_2{}^{16}O$ in the frequency range 7184–7186 $cm^{-1}$

For studying the broadening and shift of lines in the doublet the following buffer gases were used: $N_2$, Ar, He, Xe and air. An evacuated vessel of volume 5 L was degassed to a residual pressure of 3–5 mbar. Then it was filled with water vapours of natural isotope composition at a temperature of 23 °C. The pressure of water vapour inside the vessel, measured by the Elemer pressure meter, was 13–17 mbar. Then, the vessel was filled with a buffer gas to a pressure of 1 atm and the mixture was kept at rest for twenty-four hours for better mixing. For recording absorption spectra of water vapour by the procedure described above we used the cell of length 2 m.

Figure 8 shows the experimental absorption spectra of water vapour in the mixtures with various buffer gases. One can see that both the broadening and shift (the value and direction) of absorption lines depend on the kind of the buffer gas.

The spectra were approximated by using the 'hard-collision' model thoroughly described earlier. The procedure of spectrum recording included the following stages. After evacuating the analytical cell to a residual pressure of $1.3\times10^{-2}$ mbar the base line was recorded and saved, then the cell was filled with a sample gas mixture at the pressure that was continuously controlled by the Elemer pressure meter. The procedure for obtaining the optical density $D$ by using the Bouguer–Lambert–Beer law [21] was performed and the value found was accumulated over 128 samples. The results were saved to a computer memory and processed for fitting the experimental data to known model functions.

In this way, for various buffer gases the parameters of collision broadening, line shift and narrowing of the doublet lines were obtained as functions of the gas mixture pressure. These dependences are presented in Fig. 9.

The coefficients of broadening, shift and narrowing obtained after processing the line profiles are presented in Table 3 along

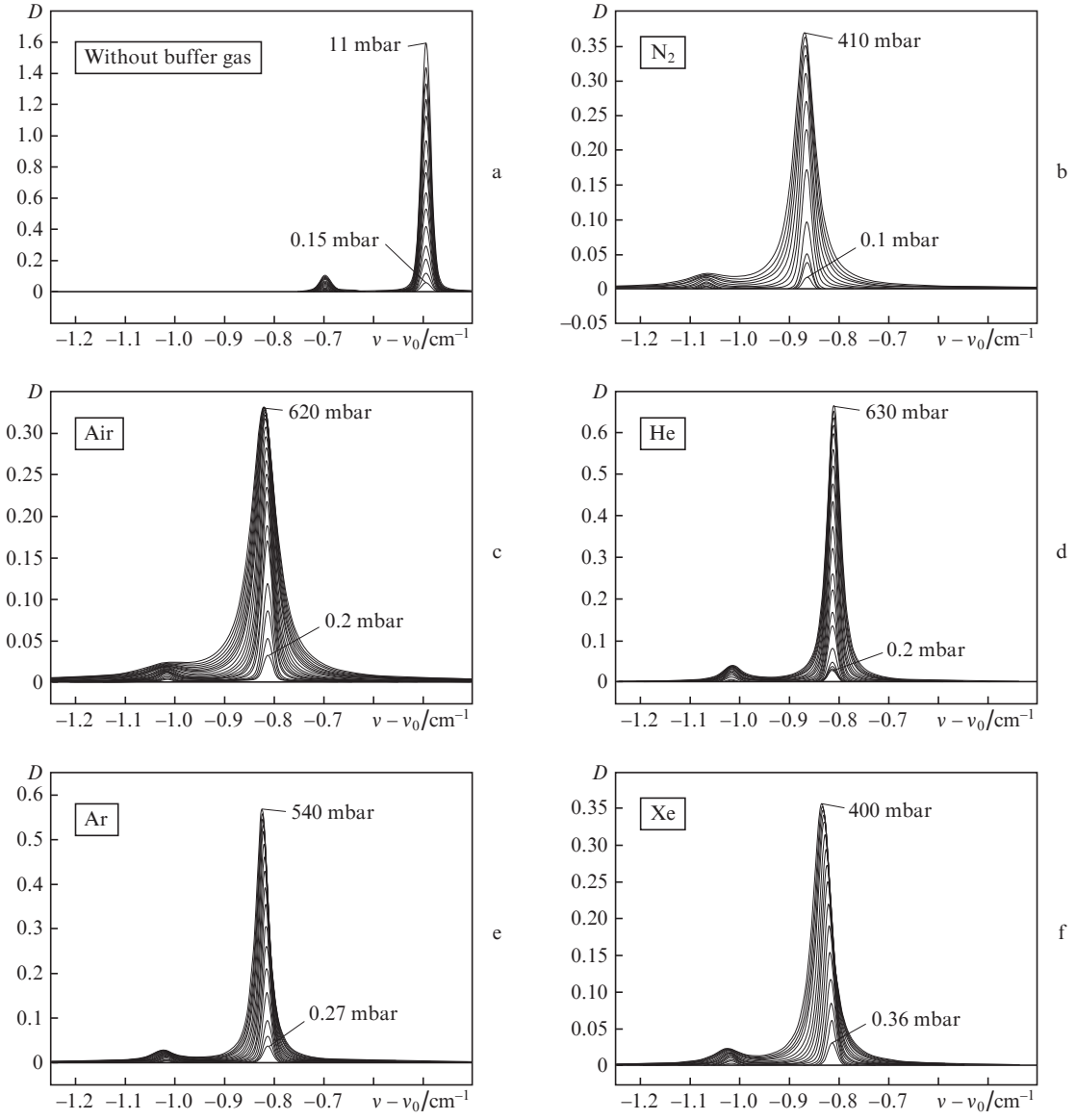


**Figure 8.** Absorption spectra of water vapour (a) without a buffer gas and in the mixtures with (b) nitrogen, (c) air, (d) helium, (e) argon and (f) xenon; the cell length is 2 m.

**Table 3.** Parameters of the line at $\nu_0$ = 7185.597 $cm^{-1}$ of the doublet of the band $\nu_1+\nu_3$ of $H_2{}^{16}O$ molecules in their collisions with molecules of various gases.

| Buffer gas | $\delta^0$/$cm^{-1}$ $atm^{-1}$ | $\gamma^0$/$cm^{-1}$ $atm^{-1}$ | | $\zeta^0$/$cm^{-1}$ $atm^{-1}$ | | $H_2O$ concentration in the mixture (%) |
|---|---|---|---|---|---|---|
| | | Present work | [4] | Present work | [4] | |
| $H_2O$ | 0.012(4) | $2.02(2)\times10^{-1}$ | $2.30(2)\times10^{-1}$ | $4.2(2)\times10^{-2}$ | — | 100 |
| He | $4.81(9)\times10^{-3}$ | $1.76(2)\times10^{-2}$ | $1.42(9)\times10^{-2}$ | $8.7(4)\times10^{-3}$ | $6(2)\times10^{-3}$ | 1.26 |
| $N_2$ | $-1.24(1)\times10^{-2}$ | $5.0(2)\times10^{-2}$ | $4.69(5)\times10^{-2}$ | $2.5(2)\times10^{-2}$ | $2.4(2)\times10^{-2}$ | 1.49 |
| Air | $-1.362(8)\times10^{-2}$ | $4.37(4)\times10^{-2}$ | — | $2.14(4)\times10^{-2}$ | — | 0.5 |
| Ar | $-2.18(1)\times10^{-2}$ | $2.20(2)\times10^{-2}$ | $1.92(4)\times10^{-2}$ | $3.4(4)\times10^{-2}$ | $3.0(2)\times10^{-2}$ | 1.24 |
| Xe | $-5.28(4)\times10^{-2}$ | $4.5(1)\times10^{-2}$ | — | $3.2(3)\times10^{-2}$ | — | 1.47 |

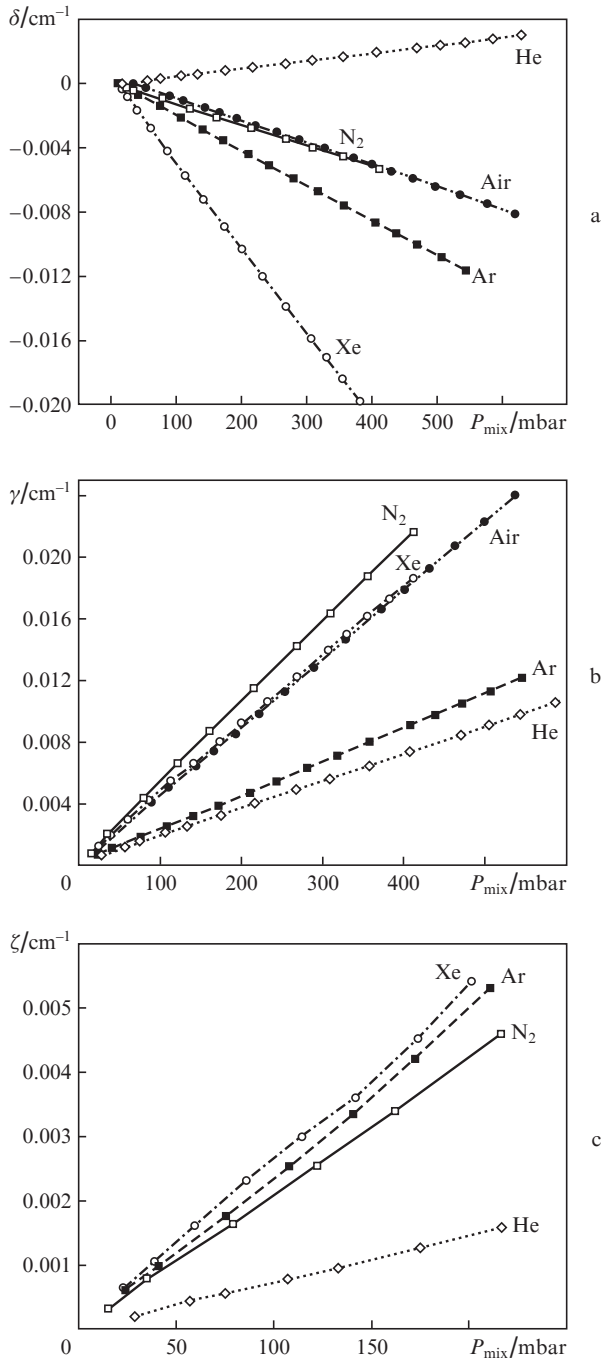


**Figure 9.** Experimental dependences of (a) the shift parameter, (b) collision broadening and (c) Dicke narrowing on the gas pressure of water vapour mixtures with various buffer gases.

with the concentrations of water vapour in the gas mixtures under study.

Broadening by xenon and argon was accompanied by the line profile asymmetry (Figs 8e and 8f), which is not taken into account by the Rautian–Sobelman profile. Seemingly, the effect of asymmetry is related to an additional, not taken into account, correlation of the fitting parameters of broadening and shift and to their dependence on relative velocities of colliding molecules [22, 23].

## 6. Conclusions

1. A two-channel DLS is created for studying absorption spectra of water vapour $H_2O$ in the near-IR range.

2. Software is developed for controlling the DLS and processing spectra (linearization, finding the central frequency and intensity of lines).

3. The allowance is made for the influence of the instrumental function of the DL, which distorts profiles of absorption spectral lines. The width of the DL generation line is found from fitting Doppler-broadened lines of $H_2O$ to theoretical profiles in the range 7184–7186 $cm^{-1}$.

4. Intensities of absorption lines of $H_2O$ are measured in the range 7184–7186 $cm^{-1}$ and compared to results of other investigations and HITRAN-2008 database.

5. The coefficients of broadening, shift and narrowing are obtained for absorption lines of $H_2O$ molecules in the range 7184–7186 $cm^{-1}$ in their collisions with various buffer gases. The effect of profile asymmetry was discovered for the absorption lines of $H_2O$ in the case of broadening by argon and xenon.

## References

1. Zobov N.F., Shirin S.V., Ovsyannikov R.I., Polyansky O.L., Barber R.J., Tennyson J., et al. *Mon. Not. R. Astron. Soc.*, **387**, 1093 (2008).
2. Liu A.W., Naumenko O., Song K.F., Voronin B., Hu S.M. *J. Mol. Spectrosc.*, **236**, 127 (2006).
3. Liu A., Naumenko O., Kassi S., Campargue A. *J. Quant. Spectrosc. Radiat. Transfer*, **110**, 1781 (2009).
4. Lepère M., Henry A., Valentin A., Camy-Peyret C. *J. Mol. Spectrosc.*, **208** (1), 25 (2001).
5. Toth R.A. *Appl. Opt.*, **33**, 4851 (1994).
6. Toth R.A., Flaud J.M., Camy-Peyret C. *J. Mol. Spectrosc.*, **67**, 206 (1977).
7. Toth R.A. *Appl. Opt.*, **33**, 4868 (1994).
8. Toth R.A. *J. Mol. Spectrosc.*, **186**, 66 (1997).
9. Leshchishina O., Mikhailenko S., Mondelain D., Kassi S., Campargue A. *J. Quant. Spectrosc. Radiat. Transfer.*, **113**, 2155 (2012).
10. Macko P., Romanini D., Mikhailenko S.N., Naumenko O.V., Kassi S., Jenouvrier A., et al. *J. Mol. Spectrosc.*, **227**, 90 (2004).
11. Toth R.A., Margolis J.S. *J. Mol. Spectrosc.*, **55**, 229 (1975).

12. http://www.elemer.ru.
13. http://www.bdsensors.ru.
14. http://jp.hamamatsu.com.
15. http://ni.com.
16. Allan D. *Proc. IEEE*, **54** (2), 221 (1966).
17. Zaslavskii V.Ya., Nadezhdinskii A.I., Ponurovskii Ya.Ya., Chernin S.M. *Kvantovaya Elektron*., **41**, 81 (2011) [*Quantum Electron*., **41**, 81 (2011)].
18. http://www.cfa.harvard.edu/hitran/.
19. Rautian S.G., Sobelman I.I. *Usp. Fiz. Nauk*, **90**, 209 (1966) [*Sov. Phys. Usp*., **9**, 701 (1967)].
20. Kuz'michev A.S., Nadezhdinskii A.I., Ponurovskii Ya.Ya. *Kvantovaya Elektron*., **41**, 650 (2011) [*Quantum Electron*., **41**, 650 (2011)].
21. Bouguer P. *Traité d'Optique sur la gradation de la lumière* (Paris: Guerin and Delatour, 1760; Moscow: Izd. Akad. Nauk SSSR, 1950).
22. Galatry L. *Phys. Rev*., **122**, 1218 (1961).
23. Ciurylo R., Pine A.S., Szudy J. *J. Quant. Spectrosc. Radiat. Transfer*, **68**, 257 (2001).